Enhanced Dielectric Properties of Ferroelectric Polymer Composites Induced by Metal-Semiconductor Zn-ZnO Core–Shell Structure

Ye Zhang,[†] Yao Wang,[†] Yuan Deng,*,[†] Mao Li,[†] and Jinbo Bai[‡]

[†]School of Materials Science and Engineering, BeiHang University, Beijing 100191, P.R. China

[‡]Laboratoire de Mécanique des Sols, Structures et Matériaux, CNRS UMR8579, Ecole Centrale Paris, Châtenay-Malabry 92290, France

S *Supporting Information*

ABSTRACT: The effect of metal-semiconductor Zn-ZnO core–shell structure on dielectric properties of polyvinylidene fluoride (PVDF) composites was investigated. Zn-ZnO fillers were obtained by the heat-treatment of raw Zn particles under air. The enhanced dielectric constant of Zn-ZnO/PVDF composites results from the duplex interfacial polarizations induced by metal-semiconductor interface and semiconductor–insulator interface. The dielectric loss is still low because of the presence of ZnO semiconductor shell between Zn metal core and insulator PVDF matrix. Furthermore, the dielectric performance of as-prepared composites could be further optimized through adjusting the thickness of semiconductor shell.

KEYWORDS: *metal-semiconductor interface, semiconductor shell, polymer composites, dielectric constant, dielectric loss*
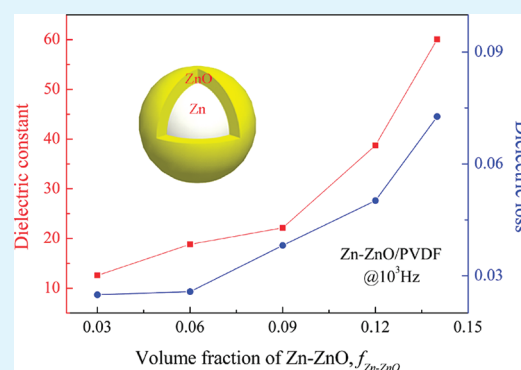
1. INTRODUCTION

Polymer-based dielectric composites with conductive fillers have potential applications in many important electric power systems[1–3] and electronic devices[4–7] because of the integrated advantage of great dielectric constant, light weight, and easy processing. Both high dielectric constant and low loss in dielectrics are desired in practical applications. Although the dielectric loss in these composites increases largely with the enhanced dielectric constant, conductive fillers do not only raise the dielectric constant obviously because of percolation theory[8–10] but also inevitably induce plenty of free charge carriers and directly cause the dramatic increase in the leakage current and conduction loss.

Recently, the metal–insulator core–shell structure has been employed to fabricate composites with high dielectric constant and low loss. The metal core is used to increase the dielectric constant due to the interfacial polarization (namely, MWS effect),[11] and the insulator shell serves as a barrier layer to control the dielectric loss effectively through blocking the electron transfer between adjacent metal cores. This type of core–shell structure is usually prepared by complicated chemical synthesis[12] or natural self-passivation.[13] The composites with chemical synthesized core–shell fillers have high dielectric constant (>100) and low loss (<0.05).[14] When the fillers is changed to Al particles with self-passivation Al_2O_3 layers outside, the corresponding composites also possess a high dielectric constant (>50) and low loss (<0.05). However, high volume fraction (>40 vol %) is necessary to achieve excellent dielectric performance above, which inevitably

introduces a lot of limitations, such as low flexibility, poor mechanical properties, etc.[15] Only few studies about metal–semiconductor core–shell fillers has been reported. Dang and co-workers employ Ag-TiO_2 core–shell structure particles to give a remarkable increase in dielectric constant of polymer composites.[16] In this letter, a Zn–ZnO core–shell structure is used as filler to significantly enhance the dielectric properties of polyvinylidene fluoride (PVDF) composites and keep low dielectric loss. The core–shell fillers are prepared by a simple heat-treatment of Zn particles under air. It is confirmed the dielectric constant of Zn–ZnO/PVDF composites is obviously increased at relatively low content due to the duplex interfacial polarization induced by both metal–semiconductor interface and semiconductor–insulator interface. Although the corresponding loss is maintained on a low level by means of the semiconductor shell, which determines the electrical properties of fillers to a considerable extent and supplies limited free charge carriers. The composite is promising dielectric materials to apply in many modern electronic devices.
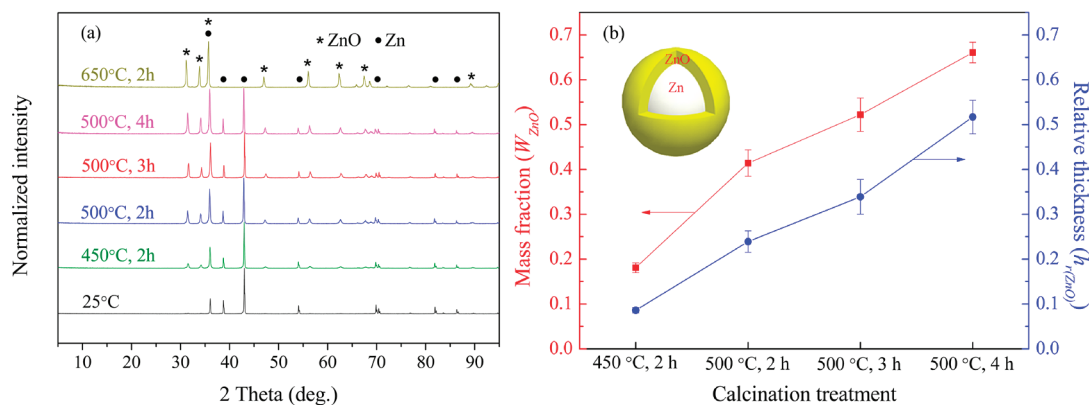
2. EXPERIMENTAL SECTION

Raw microscale Zn particles were calcinated under ambient atmosphere at 450–500 °C for 2–4 h, and then ZnO was formed on the surface of Zn sphere to obtain Zn–ZnO core–shell structure. The thickness of ZnO shell was tuned by
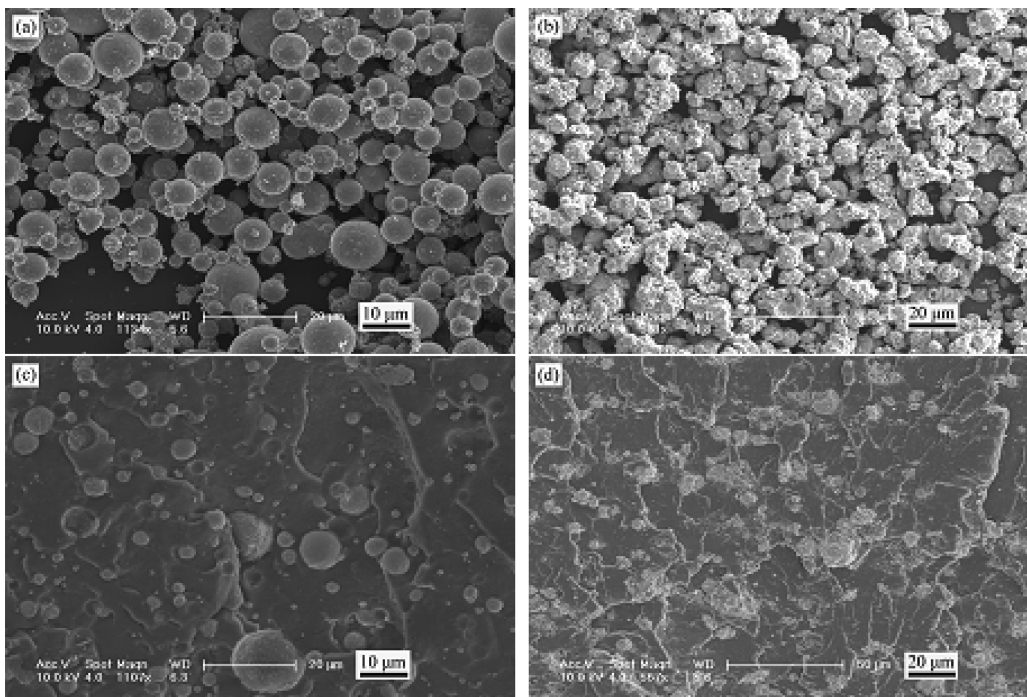
Figure 1. (a) XRD patterns of Zn particles under different calcination conditions. (b) Relationship of ZnO shell mass fraction (W_{ZnO}) and relative thickness ($h_{r(ZnO)}$) correspond to different calcination conditions, the inset is the scheme of Zn−ZnO core−shell structure.


Figure 2. SEM images of (a) raw Zn particles; (b) Zn−ZnO core−shell particles obtained from calcination at 500 °C for 3 h; cross-section images of (c) Zn/PVDF and (d) Zn-ZnO/PVDF composites with filler content of 0.14.

adjusting calcination temperature and time. Subsequently, Zn−ZnO/PVDF composites with volume fraction of Zn−ZnO core−shell fillers (f_{Zn-ZnO}) varying from 0 to 0.16 were prepared through the method of flocculation. As for composites containing fillers with different ZnO shell thickness, they were marked based on corresponding calcination condition and listed as follows: C1 (450 °C, 2 h), C2 (500 °C, 2 h), C3 (500 °C, 3 h), and C4 (500 °C, 4 h). The phase was identified with X-ray diffraction with CuKa radiation (Rigaku D/MAX-2200 diffractometer, Japan). The microstructure of the composites was observed with a scanning electron microscopy (SEM, FEI Sirion 200). All samples were painted with silver paste on both sides prior to dielectric measurement by using an impedance analyzer (Agilent 4294A) over frequency range from 1×10^2 to 1×10^7 Hz.

3. RESULTS AND DISCUSSION

When raw microscale Zn particles were calcinated under air, ZnO was formed on the surface of Zn sphere to obtain Zn-ZnO core−shell structure. As seen in Figure 1a, the XRD patterns can be indexed to Zn (PDF: 65−3358) and ZnO (PDF: 65−3411), respectively. On the other hand, the normalized intensities in XRD spectra revealed the content of ZnO shell was increased gradually from 450 to 500 °C. When Zn particles were calcinated at 650 °C for 2 h, no crystal Zn was detected, indicating Zn has been oxidized into ZnO completely.

Figure 1b displays the variation of ZnO shell mass fraction (W_{ZnO}) and relative thickness ($h_{r(ZnO)}$) with calcination treatment. W_{ZnO} is calculated by direct comparison method in XRD quantitative analysis,[17] and the related equation is listed below
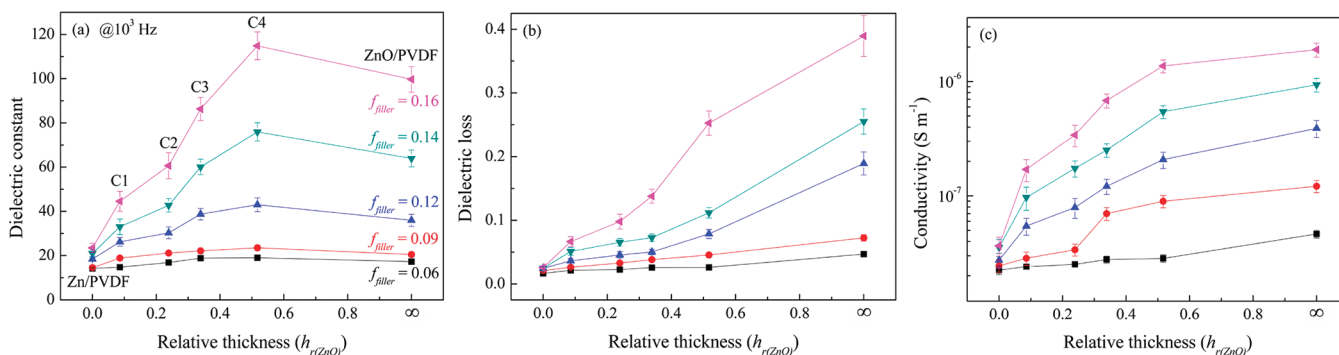
Figure 3. (a) Dielectric constant, (b) dielectric loss, and (c) conductivity of Zn/PVDF, Zn-ZnO/PVDF (C1−C4), and ZnO/PVDF composites with different volume fraction of fillers (f_{filler}) as a function of relative thickness ($h_{r(ZnO)}$) measured at 1×10^3 Hz.
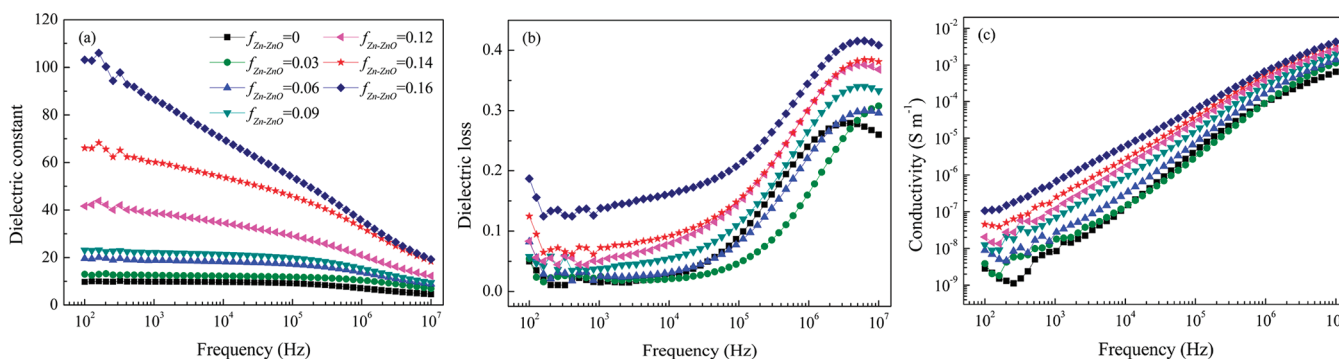
Figure 4. (a) Dielectric constant, (b) dielectric loss, and (c) conductivity of composites C3 with different filler content as a function of frequency.

$$W_{ZnO} = \frac{\dfrac{I_{ZnO}}{(I_{ZnO})_0}\mu_{m(Zn)}}{\dfrac{I_{ZnO}}{(I_{ZnO})_0}(\mu_{m(Zn)} - \mu_{m(ZnO)}) + \mu_{m(ZnO)}} \quad (1)$$

where I_{ZnO} and $(I_{ZnO})_0$ denote the intensities of the same lines for ZnO shell and pure ZnO, respectively, $\mu_{m(Zn)}$ and $\mu_{m(ZnO)}$ are the constants standing for mass absorption coefficients of ZnO and Zn.

While $h_{r(ZnO)}$, defined as $(r_2 - r_1)/r_1$, can be determined by the equation below

$$\frac{m_{Zn}}{m_{ZnO}} = \frac{r_1^3 \rho_{Zn}}{(r_2^3 - r_1^3)\rho_{ZnO}} \quad (2)$$

where m_{Zn} and m_{ZnO} are the weights of Zn core and ZnO shell, ρ_{Zn} and ρ_{ZnO} represent the densities of Zn and ZnO, and r_1 and r_2 denote the radii of Zn core and Zn−ZnO core−shell, respectively. Then

$$h_{r(ZnO)} = \frac{r_2 - r_1}{r_1}$$
$$= \left(\frac{m_{ZnO}\rho_{Zn} + m_{Zn}\rho_{ZnO}}{m_{Zn}\rho_{ZnO}}\right)^{1/3} - 1 \quad (3)$$

As shown in Figure 2a, b, the surface of raw Zn particles is smooth and the sizes of diameter are about 2−10 μm. When those raw Zn powders are calcinated at 500 °C for 3 h, the diameters of Zn−ZnO core−shell particles increase to 5−20 μm. Furthermore, the surface of the core−shell particle became rough obviously. When the Zn−ZnO core−shell particles or raw Zn powders are mixed with PVDF to give complexes, Zn−

ZnO or ZnO particles are homogeneously dispersed in PVDF matrix (shown in Figure 2c, d and Figure S1 in the Supporting Information). It is beneficial to increasing the dielectric constant and decreasing the loss and conductivity of corresponding composites.

Variation of dielectric properties of PVDF composites at different volume fraction of fillers (f_{filler}) with relative thickness of ZnO shell ($h_{r(ZnO)}$) is shown in Figure 3. As seen in Figure 3a, the dielectric constant at 10^3 Hz for $h_{r(ZnO)}$ between 0 and ∞ is always higher than that of $h_{r(ZnO)} = 0$ at the same f_{filler}. That means the Zn−ZnO/PVDF composites possess larger dielectric constant compared to the Zn/PVDF composites, which can be ascribed to the duplex interfacial polarizations induced by metal−semiconductor interface and semiconductor−insulator interface. While the Zn particles, with natural insulating self-passivation layers outside,[18] are thought to cause relatively weak interfacial polarization. The dielectric constant increased with the increase of $h_{r(ZnO)}$. It is considered that the interfacial area in composites increases gradually with the increase of $h_{r(ZnO)}$ because fo the volume expansion, which enhances the duplex interfacial polarizations and endows composites with higher and higher dielectric constant. However, when $h_{r(ZnO)}$ arrived at ∞, the dielectric constant was decreased at any content, which might be attributed to the weakened interfacial polarization in ZnO/PVDF composites due to the disappearance of metal−semiconductor interface.

As far as the dielectric loss and conductivity are concerned, Figure 3b, c clearly show that they have similar tendency of change with the $h_{r(ZnO)}$. The dielectric loss for $h_{r(ZnO)}$ between 0 and ∞ is higher than that of $h_{r(ZnO)} = 0$. The dielectric loss of polymer composites filled with conductors or semiconductors is closely related with fillers in the low frequency range, which possess relatively good electrical properties and can provide lots

of free charge carriers so as to cause high leakage current.[19,20] However, for conductive fillers coated with semiconductor shells outside, the shells are usually considered to have dramatic effect on the electrical properties of fillers and their composites.[21] Therefore, in our case, the electrical properties of Zn−ZnO/PVDF composites are higher than that of Zn/PVDF composites(shown in Figure 3c). Subsequently, the dielectric loss and conductivity of complexes with different thickness of shells were further increased with $h_{r(ZnO)}$ (see Figure 3b, c), which can be attributed to the increasing electrical properties with the semiconductor shell thickness.

It is interesting to note that the composites C3 manifested the best dielectric properties among the six different composites due to a rapid increase in dielectric constant and keep in low loss. Especially, the composite with $f_{Zn−ZnO} = 0.14$ in C3 is suitable for embedded capacitor application owing to high dielectric constant of 60 and low loss of 0.07. As seen in Figure 4a, it is found that in the low frequency range ($<1 \times 10^4$ Hz), the dielectric constant of composites C3 with $f_{Zn−ZnO}$ below 0.16 decreases slowly with the increase of frequency, indicating relatively weak frequency dependence in the frequency and content range. Furthermore, the corresponding loss could be stabilized at a low level, which is benefited from the semiconductor shell (see Figure 4b). As for the electrical properties, Figure 4c displays the conductivity of composites C3 increases almost linearly with increasing frequency, indicating a good electrical insulation performance of C3 in the content range.[22]

4. CONCLUSIONS

Metal-semiconductor Zn−ZnO core−shell structure was fabricated by a simple calcination process of raw Zn particles, and uniformly distributed in PVDF matrix owing to the fabrication way of flocculation. The relatively high dielectric constant and low loss in Zn-ZnO/PVDF composites are benefitted from the metal-semiconductor core−shell structure, which introduces the duplex interfacial polarizations and a small amount of free charge carriers. With the increase of relative thickness of ZnO shell ($h_{r(ZnO)}$), the dielectric constant and loss of the composites were increased further. However, it is found the composites C3 presented the best dielectric properties in the present study due to a fast increase in dielectric constant and keep low loss. Especially, the composite with $f_{Zn−ZnO} = 0.14$ possesses a high dielectric constant of 60 and low loss of 0.07, which can be applied in embedded passive components and other related electronic devices.

■ ASSOCIATED CONTENT

Ⓢ Supporting Information
Cross-section SEM images (PDF). This material is available free of charge via the Internet at http://pubs.acs.org.

■ AUTHOR INFORMATION

Corresponding Author
*E-mail: dengyuan@buaa.edu.cn.

■ ACKNOWLEDGMENTS

■ REFERENCES

(1) Zhou, T.; Zha, J. -W.; Hou, Y.; Wang, D. R.; Zhao, J.; Dang, Z. -M. *ACS Appl. Mater. Inter.* **2011**, *3*, 4557−4560.

(2) Putson, C.; Lebrun, L.; Guyomar, D.; Muensit, N.; Cottinet, P. -J.; Seveyrat, L.; Guiffard, B. *J. Appl. Phys.* **2011**, *109*, 024104.

(3) Lu, J. X.; Moon, K. S.; Kim, B. K.; Wong, C. P. *Polymer* **2007**, *48*, 1510−1516.

(4) Dimiev, A.; Lu, W.; Zeller, K.; Crowgey, B.; Kempel, L. C.; Tour, J. M. *ACS Appl. Mater. Inter.* **2011**, *3*, 4657−4661.

(5) Liu, H. Y.; Shen, Y.; Song, Y.; Nan, C. -W.; Lin, Y. H.; Yang, X. P. *Adv. Mater.* **2011**, *23*, 5104−5108.

(6) Srivastava, R. K.; Narayanan, T. N.; Mary, A. P. R; Anantharaman, M. R.; Srivastava, A.; Vajtai, R.; Ajayan, P. M. *Appl. Phys. Lett.* **2011**, *99*, 113116.

(7) Thomassin, J. M.; Huynen, I.; Jerome, R.; Detrembleur, C. *Polymer* **2010**, *51*, 115−121.

(8) Dang, Z. M.; Yuan, J. K.; Zha, J. W.; Zhou, T.; Li, S. T.; Hu, G. H. *Prog. Mater. Sci.* **2011**, DOI: 10.1016 /j.pmatsci. 2011.08.001.

(9) Nan, C. -W.; Shen, Y.; Ma, J. *Annu. Rev. Mater. Res.* **2010**, *40*, 131−151.

(10) Wang, G. S. *ACS Appl. Mater. Inter.* **2010**, *2*, 1290−1293.

(11) He, F.; Lau, S.; Chan, H. L.; Fan, J. T. *Adv. Mater.* **2009**, *21*, 710−715.

(12) Qi, L.; Lee, B. I.; Chen, S.; Samuels, W. D.; Exarhos, G. J. *Adv. Mater.* **2005**, *17*, 1777−1781.

(13) Zhou, Y.; Wang, H.; Xiang, F.; Zhang, H.; Yu, K.; Chen, L. *Appl. Phys. Lett.* **2011**, *98*, 182906.

(14) Shen, Y.; Lin, Y.; Li, M.; Nan, C. -W. *Adv. Mater.* **2007**, *19*, 1418−1422.

(15) Xu, J. W.; Moon, K. S.; Tison, C.; Wong, C. P. *IEEE Trans. Adv. Packag.* **2006**, *29*, 295−306.

(16) Dang, Z. -M.; You, S. -S.; Zha, J. -W.; Song, H. -T.; Li, S. -T. *Phys. Status Solidi A* **2010**, *207*, 739−742.

(17) Cullity, B. D.; Stock, S. R. *Elements of X-Ray Diffraction*, 3rd ed.; Prentice Hall: Upper Saddle River, NJ, 2001.

(18) Porter, F. C. In *Corrosion Technology*, 1st ed.; Schwietzer, P. A., Ed.; Marcel Dekker: New York, 1994; Vol. 6, p 121.

(19) Yuan, J. -K.; Dang, Z. -M.; Yao, S. -H.; Zha, J. -W.; Zhou, T.; Li, S. -T.; Bai, J. B. *J. Mater. Chem.* **2010**, *20*, 2441−2447.

(20) Deng, Y.; Li, N.; Wang, Y.; Zhang, Z. W.; Dang, Y.; Liang, J. Y. *Mater. Lett.* **2010**, *64*, 528−530.

(21) Xu, J. W.; Wong, C. P. *Appl. Phys. Lett.* **2005**, *87*, 082907.

(22) Chang, C. -M.; Liu, Y. -L. *ACS Appl. Mater. Interfaces* **2011**, *3*, 2204−2208.